Single-Molecule Study of Lateral Mobility of Epidermal Growth Factor Receptor 2/HER2 on Activation

Zeyu Xiao,[†] Xinyong Ma,[†] Yaxin Jiang,[†] Zilong Zhao,[†] Bo Lai,[‡] Jieying Liao,[‡] Jiachang Yue,[‡] and Xiaohong Fang*[,†]

Beijing National Laboratory for Molecular Sciences, Institute of Chemistry, Chinese Academy of Sciences, Beijing, China, 100080, and Institute of Biophysics, Chinese Academy of Sciences, Beijing, China, 100101

Received: October 25, 2007; In Final Form: January 8, 2008

The transmembrane protein HER2, a member of the epidermal growth factor receptor family of tyrosine kinase, plays important roles in many fundamental cellular processes as well as the pathogenesis of many cancers. In this work, we have applied the single-molecule fluorescence microscopic method to study lateral mobility change of HER2 on activation by imaging and tracking individual GFP-tagged HER2 molecules on the membrane of living cells. The single HER2 molecules displayed different diffusion rates and modes. It was interesting to find that the mobility of HER2 increased upon stimulation by heregulin β1, the specific ligand of HER3. The faster diffusion was related to the tyrosine phosphorylation of HER2 or EGFR. The results provided new information for the understanding of HER2 activation and molecular mechanism of signal transduction through HER2/HER3 heterodimerization.

Introduction

The receptor tyrosine kinase HER2 or erbB2 is a member of the epidermal growth factor receptor (EGFR or erbB1) family, which also includes HER3/erbB3 and HER4/erbB4. The erbB family proteins are engaged in an extensive network of homo- and hetero-associations regulating many important biological processes such as development, cell proliferation, apoptosis, differentiation and oncogenesis.[1] HER2 plays a critical role in the cellular effects of the erbB receptor network. The significance of HER2 is underscored by its overexpression in many types of cancers, e.g., about 30% of breast carcinomas, and its overexpression is associated with poor prognosis.[2,3]

As the only ligand orphan receptor in erbB family, HER2 is activated by heterodimerization with another ligand-activated erbB receptor. The HER2 kinase amplifies the signal by modulating receptor internalization and prolonging signal transduction. Recent years have witnessed increasing interest in the study of HER2 activation through its complexing with HER3, since HER2/HER3 is the most representative heterodimer found in breast cancer.[4] HER3 is a kinase-defective protein. It is known that upon binding to its ligand, such as heregulin β1 (HRG), HER3 heterodimerizes with either HER2 or EGFR, and the constitution of HER2/HER3 is preferential. This leads to the phosphorylation of HER2 or EGFR receptor, the coupling of other intracellular downstream mediators, and the activation of the signal pathways of PI3K (phosphatidylinositol 3-kinase), MAPK, etc. Although previous studies have shown that the signal pathways activated by HER2/HER3 are involved in the proliferation, survival, adhesion, and motility of tumor cells, the molecular mechanism and biological consequences of HER2/HER3 association are not yet completely known.[5] Efforts have been made to apply a variety of biochemical assays, which were mainly carried out in vitro with fixed cells, cell lysates, or purified recombinant proteins, to study the molecular interaction of HER2 with HER3 and HER2 activation.[6−9]

Single-molecule fluorescence microscopy has been recently developed as a new tool for biomolecular study not only in vitro but also in living cells.[10−17] It provides information on the spatial and temporal heterogeneity of molecules which may be obscured by the averaging in conventional ensemble biochemical experiments. Single-molecule tracking of proteins in living cells is becoming a powerful method to study protein local environments and interactions that constrain their mobility. Many single molecule studies on signaling receptors have offered new insights into their localization, assembly, and activation during the singal transduction process.[18−26] In these studies, a decrease in receptor lateral mobility after receptor activation is usually observed. For example, single-molecule imaging of small G protein Ras revealed that Ras diffusion slowed down on activation.[18] It indicated the formation of large Ras-signaling complexes, which provided a platform for transducing Ras signal to effector molecules. Douglass et al. reported that during T cell signaling, the plasma membrane microdomains, which were created by the clustering of the coreceptor CD2, adaptor protein LAT, and tyrosine kinase Lck, concentrated or excluded other cell surface proteins.[19] This led to a significant reduction in single-molecule LAT diffusion. We recently investigated the effect of lipid rafts on transforming growth factor TGFβ1 signaling.[26] The reduced diffusion of individual TGFβ type I receptors (TβR1) after TGFβ1 stimulation reflected their heteromeric assembly with type II receptors.

In this work, we studied the diffusion dynamics of HER2 when it is heterodimerized with HER3 by single-molecule imaging and tracking of HER2 in living cells. The plasmid of GFP-tagged HER2 was constructed, and the individual HER2-GFP molecules expressed on the cell surface were monitored before and after they were activated by HRG, the specifc ligand of HER3. The coupling of GFP to HER2 provided an easy way to achieve single-dye labeling of HER2 and obtain information

* To whom correspondence should be addressed. Phone: +86-10-62650024. Fax: +86-10-62650024. E-mail: xfang@iccas.ac.cn.
[†] Institute of Chemistry, Chinese Academy of Sciences.
[‡] Institute of Biophysics, Chinese Academy of Sciences.

10.1021/jp710302j CCC: $40.75
Published on Web 03/07/2008

on extracellular ligand stimulation. Interestingly, unlike other reported membrane receptors with decreased mobility upon activation, we found that HER2 molecules diffused faster after HRG treatment. Further analysis indicated the increased movement was related to tyrosine phosphorylation of HER2 or EGFR, the two HER3 dimerization partners. The living cell single-molecule analysis offered a valuable approach to better understanding of HER2 activation and signal transduction mechanism of HER2/HER3.

Experimental Section

Plasmid Construction. The DNA fragments encoding full-length HER2 were subcloned from pcDNA3.1/CT-GFP-TOPO into Kpn I/Sma I sites of pGFP-N1 (Clontech) to obtain HER2-GFP expression vectors.

Cell Culture and Transfection. The MCF-7 breast tumor cell line, a gift from Professor Qinwei Yin (Institute of Biophysics, Chinese Academy of Sciences, People's Republic of China), was grown on glass-bottom culture dishes (MatTek Co.) in pH 7.4 RPMI1640 (Gibco BRL, Grand Island, NY) supplemented with 10% fetal calf serum (HyClone Logan, UT), 100 units/mL penicillin, 100 μg/mL streptomycin, and 5% carbon dioxide at 37 °C. Subconfluent cells were transfected with HER2-GFP expression vectors using Lipofectamin2000 (Invitrogen). In all experiments, cells transiently expressing GFP-tagged proteins were used. The expression levels in each experiment were closely matched. All the cells were serum-starved in the phenol red-free medium for 24 h before drug application and fluorescence imaging. The cells were kept in this serum-free medium during the drug treatment and imaging.

Drug Application. All the reagents used for the cell treatment including heregulin β1 (HRG), AG1478, and AG825 were purchased from Sigma (St. Louis, MO). The addition of the reagent to the cell culture medium was carried out under a dark condition. 10 nM HRG was used to stimulate the cells at 37 °C 5 min before the microscopy observation. 50 μM AG825, the specific tyrosine kinase inhibitor of HER2, and/or100 μM AG1478, the specific tyrosine kinase inhibitor of EGFR,[27,28] were added into the medium an hour prior to the addition of HRG when needed. 10 μg/mL anti-HER3 monoclonal antibody (NeoMarkers, Fremont, CA) was used to inhibit heregulin β1 binding to HER3.[29] Destabilization of cell cytoskeleton was achieved by 30-min incubation at 37 °C in the medium supplemented with 0.5 μM LatrunculinB (Calbiochem, San Diego, CA).[30]

Single-Molecule Fluorescence Imaging. An objective-type total internal reflection fluorescence microscope, which was based on an inverted microscope (IX-71, Olympus) with a total internal reflective fluorescence illuminator and a 100× oil-immersion objective (Olympus, Japan,NA1.45) was used for single-molecule fluorescence imaging. The 488-nm laser line from an argon ion laser (Melles Griot, USA) was used to excite GFP. Fluorescence signals were collected by the objective and passed through two filters, BA510IF long pass filter (Chroma, USA) and HQ525/50 band-pass filter (Chroma, USA), before directed to an intensified CCD camera (I-Pentamax EEV 512 × 512 FT, Roper Scientific, USA). Images were acquired with 100-ms exposure time and analyzed with MetaMorph6.1 software (Molecular Devices Corp., USA)

Imaging of GFP on Coverslips. Single molecule fluorescence imaging of GFP on coverslips was performed as a control experiment for that of HER2-GFP on living cell surface. GFP protein purified from *E. coli* was first dissolved in a high salt buffer (600 mM NaCl, 150 mM PBS buffer, pH 7.4) to prevent dimer formation and then immobilized on the coverslips through biotinylated GFP antibody (Clontech) using the method reported previously.[13] Those fluorescence spots of GFP whose size were within the diffraction limit (2 × 2 pixels, 460 nm × 460 nm) and bleached in a single step were identified as single GFP molecules.

Mobility Analysis of Single Molecules. Time-lapse series of single HER2-GFP images were taken up to 200 images per sequence. The positions of individual fluorescent HER2-GFP molecules were determined in each image, and the two-dimensional trajectories of these molecules in the plane of the basal membrane were reconstructed by MetaMorph6.1 software (Molecular Devices Corp., USA). For the calculation of diffusion coefficient, we plotted the mean square displacement (MSD) from each trajectory against time (t).[25] For each molecule, the slope of the first four time points in the MSD-t plot was used to calculate the diffusion coefficient according to the equation $MSD_{t\to 0} = 4Dt$.[25,26] The distributions of HER2 diffusion coefficients were obtained under different conditions (different cell treatments), and each distribution histogram represented the data from 106 to 158 single HER2 molecules in 10−15 cells. Those exhibiting $D_{100ms} < 0.01167$ $\mu m^2/s$ (derived by the Gaussian fitting to the data on single GFP molecules on glass as a 95 percentile point) were defined as immobile molecules under our microscopic resolution.[26] Moreover, the confinement length (L) of HER2 in different conditions was calculated by plotting the overall change of MSD of all single molecules vs time from 100 ms to 2 s and then fitting the curve according to the equation below,[31] where $r^2(t)$ is the time dependence of mean MSD and D is the mean diffusion coefficient

$$r^2(t) = \frac{L^2}{3}\left(1 - \exp\left(\frac{-12Dt}{L^2}\right)\right)$$

Results and Discussion

Single-Molecule Imaging of HER2 in Living Cells. As shown in Figure 1, we achieved single-molecule fluorescence imaging of HER2-GFP expressed on the membrane of MCF-7, a model cell line extensively used to study erbB family signal transduction.[8,32] The expression level of HER2-GFP was kept low, so individual HER2 molecules could be observed as well-dispersed fluorescent spots by TIRFM (Figure 1A). The fluorescent spots that displayed the size within the diffraction limit (2 × 2 pixels, 460 nm × 460 nm) and the characteristics of one-step photobleaching (Figure 1C) were identified as single HER2 molecules followed for later diffusion tracking. The collected single HER2-GFP molecules were also fluorescent more than 10 image frames to exclude the background noise and ensure the diffusion coefficient analysis. The intensity distribution of those single HER2- GFP molecules was similar to that of single purified GFP molecules imaged on the coverslips (Figure 1B), confirming the single HER2 imaging on cell membrane.[18,25]

Analysis of HER2 Diffusion in the Resting State. On the basis of the consecutive images of the single HER2 molecules on the basal membrane of the cells, the diffusion trajectories of each molecule were obtained (Figure 2A). The MSD changes over time for each trajectory were plotted (shown as Figure 2B) and the diffusion coefficients (D) of individual HER2 molecules were derived. Different molecules showed different diffusion characteristics. The majority (~89%) of the molecules were mobile, and most of them displayed restricted diffusion (Figure 2, trajectory 2) as previously reported.[25] However, a few molecules (~11%) were found immobile, and some mobile

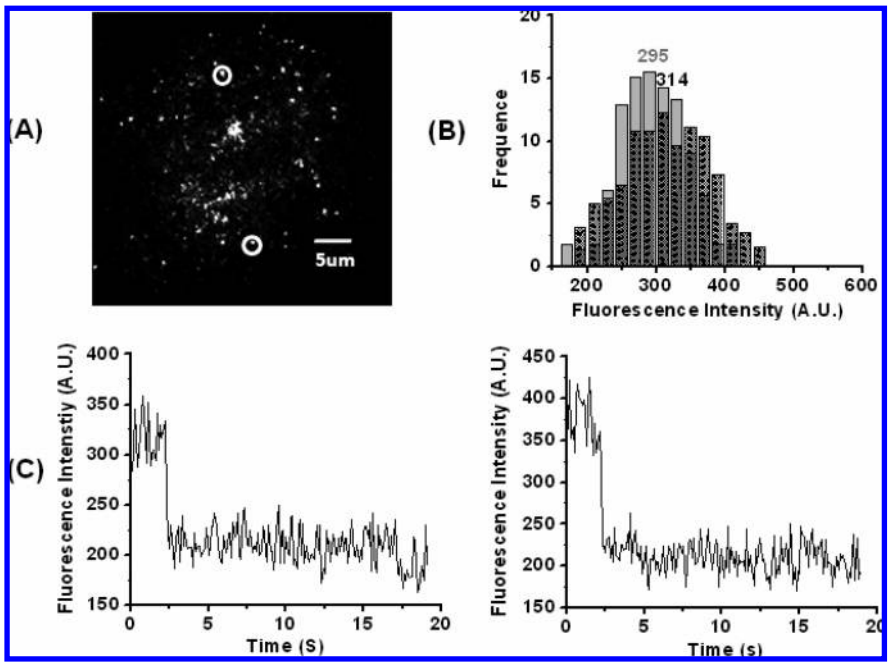

Figure 1. (A) Single-molecule fluorescence imaging of HER2-GFP on the living cell membrane. Scale bar: 5 μm. (B) Fluorescence intensity distributions of individual HER2-GFP spots on the living cell membrane (dashed dark bar) and single GFP molecules on the coverslips (light gray bar). The histograms were generated from 260 HER2-GFP molecules on the cells and 232 GFP molecules on the coverslips. (C) Fluorescence intensity trajectories of two typical single HER2-GFP molecules shown by the circles in part A displaying typical one-step photobleaching.

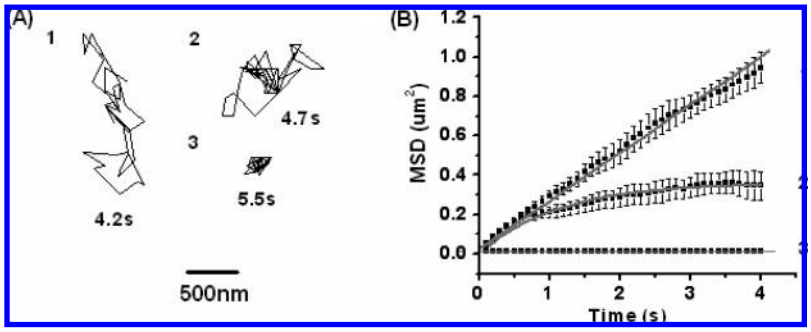

Figure 2. (A) Illustrative examples of single HER2 molecules with different diffusion trajectories. (B) Plots of the MSD vs time for the three trajectories shown in part A.

molecules (22%) appeared as simple diffusion (Figure 2, trajectory 1) judged from their trajectories and MSD-*t* curves.[18,19] The diffusion coefficient distribution of all the single HER2 molecules was shown in Figure 3A with the mean value at 0.055 μm^2/s.

Orr et al. recently reported the single-molecule diffusion of EGFR and HER2 under different conditions of cholesterol contents to study the association of lipid rafts with the two receptors.[25] They used AF-546 dye labeled antibodies to monitor EGFR and HER2 (e.g., Fab fragment of mAb 7C2 for HER2) in HME184A1 cell, and calculated the change of overall MSD of all single molecules in 4 s of observation. They suggested the diffusion of HER2 was restricted with the *D* of 0.035 μm^2/s. In our work of tracking GFP-tagged HER2, we calculated the change of MSD with time for each molecule and found that the molecules may display more diffusion modes. The mean value derived from our single-molecule *D* distribution was a little larger than that Orr reported. Worth mentioning is that most of individual HER2-GFP could only be tracked for about 2−4 s before photobleaching. In Figure 2, the molecules with fluorescent time longer than 4 s (about 12% of single HER2-GFP molecules) were selected to compare the reported result from 4 s of observation by the dye labeling.[25] The short fluorescent time of GFP did not affect the calculation of diffusion coefficient (*D*) as only the first four time points (0−400 ms) in the MSD *t* plot were used for calculation. If we used the statistical method as they did and plotted the overall MSD change of our single molecules against time (see Supporting Information), it could also result in the curve fitting for the restriction mode.[25] However, the derived diffusion coefficient (0.055 ± 0.0030 μm^2/s) was still a little larger than they reported. Besides the difference in labeling strategy, different diffusion coefficient may be due to the study of HER2 in different cell lines.[33] In our experiment, the average diffusion coefficient (0.055 ± 0.0035 μm^2/s) as well as the diffusion distribution of HER2 all fell within the range of reported diffusion coefficients of membrane proteins, which were from 0.005 to 0.5 μm^2/s.[18,19,22−24,34] Moreover, we just compared the relative mobility of HER2 before and after HRG acitivation in the same cell batch for the later study.

Faster Diffusion of HER2 on HRG Activation. It is known that the activation of HER2 can be achieved by the administration of HRG, which binds specifically to HER3 and promotes the heterodimerization of HER3 with HER2. As there existed relatively high levels of endogenous HER3 in the cell line we used,[8] we then monitored the diffusion of single HER2 molecules after HRG activation and compared their diffusion behavior to that in the resting cells.

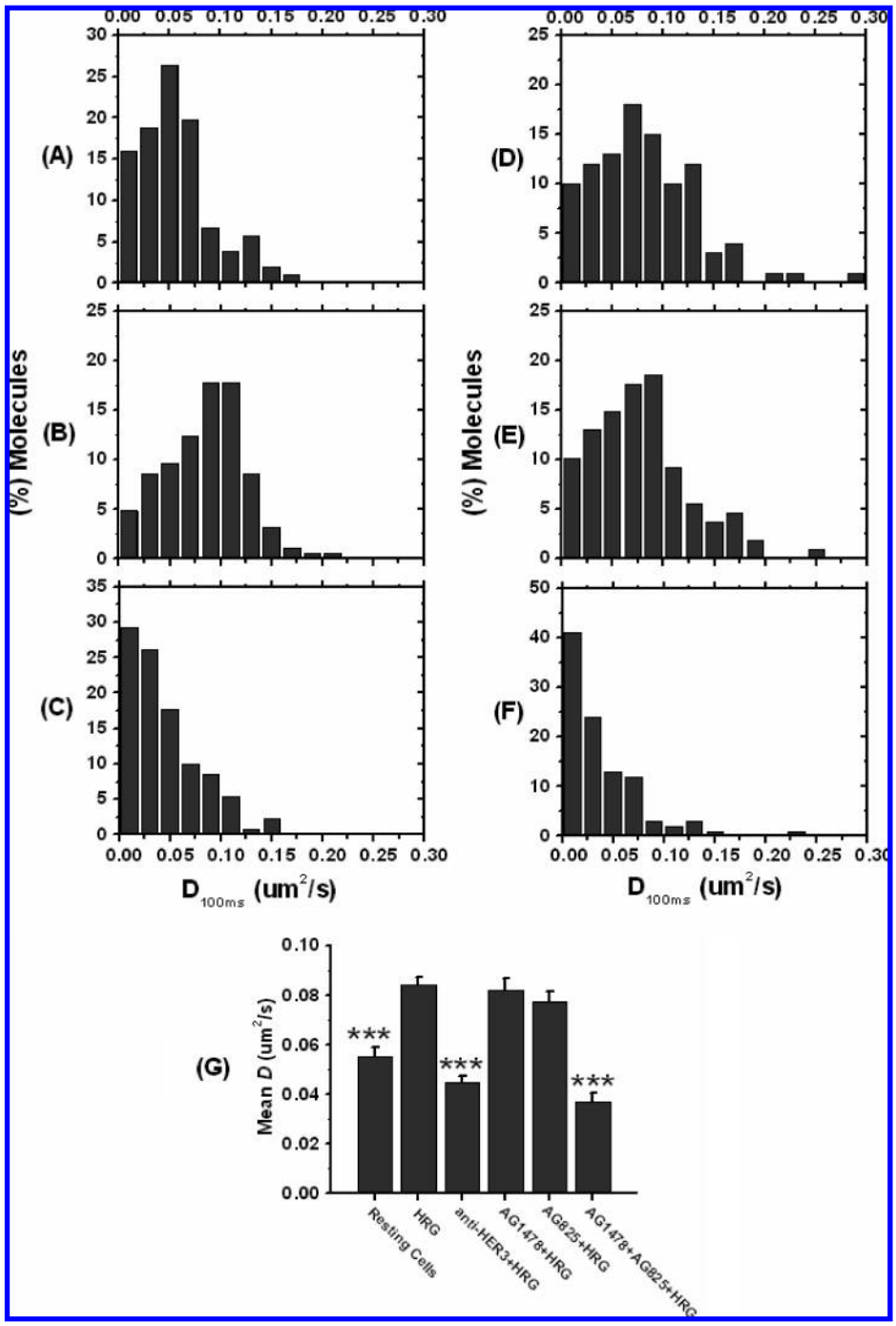

Figure 3. (A−F) Distributions of HER2 diffusion coefficients under different conditions: (A) resting cells, (B) after HRG stimulation, (C) treating with anti-HER3 monoclonal antibody before adding HRG, (D) treating with EGFR phosphorylation inhibitor AG1478 before adding HRG, (E) treating with HER2 phosphorylation inhibitor AG825 before adding HRG, and (F) treating with both EGFR phosphorylation inhibitor AG1478 and HER2 phosphorylation inhibitor AG825 before adding HRG. The mean values for A−F is 0.055 ± 0.0035, 0.085 ± 0.0032, 0.045 ± 0.0031, 0.082 ± 0.0051, 0.077 ± 0.0047, and 0.037 ± 0.0038 $\mu m^2/s$, separately. (G) Mean diffusion coefficients of HER2 obtained from the *D* distribution histograms shown in A−F. There is a significant statistical difference in diffusion coefficient values between A and B ($p < 0.001$), B and C ($p < 0.001$), B and F ($p < 0.001$). No significant difference was found between B and D ($p > 0.05$) and B and E ($p > 0.05$).

As shown in parts A and B of Figure 3, there was an apparent increase in HER2 diffusion upon stimulation. The immobile molecules could be hardly found. The distribution of the diffusion coefficients shifted to the higher values with the mean at 0.085 ± 0.0032 $\mu m^2/s$, which were larger than those in the resting state with the mean at 0.055 ± 0.0035 $\mu m^2/s$ ($p < 0.001$ in the student's *t* test for the two groups of *D*).

We have also calculated the averaged length of confinement domain of HER2.[31] It also increased upon HRG stimulation (from 0.64 ± 0.018 to 0.96 ± 0.029 μm). Therefore, unlike other reported signaling receptors,[18,19,26] HER2 moved faster and more freely on activation.

We further confirmed that the faster diffusion of HER2 was due to HRG stimulation using anti-HER3 monoclonal antibody Ab-5. This antibody has been reported to inhibit the binding of HRG to HER3 without affecting the cell growth.[29] As shown in parts C and B of Figure 3, in the presence of the antibody, D_{100ms} distribution after HRG treatment (mean value at 0.045 ± 0.0031 $\mu m^2/s$) shifted back to the resting level, and the confinement domain shifted back to 0.54 ± 0.014 μm.

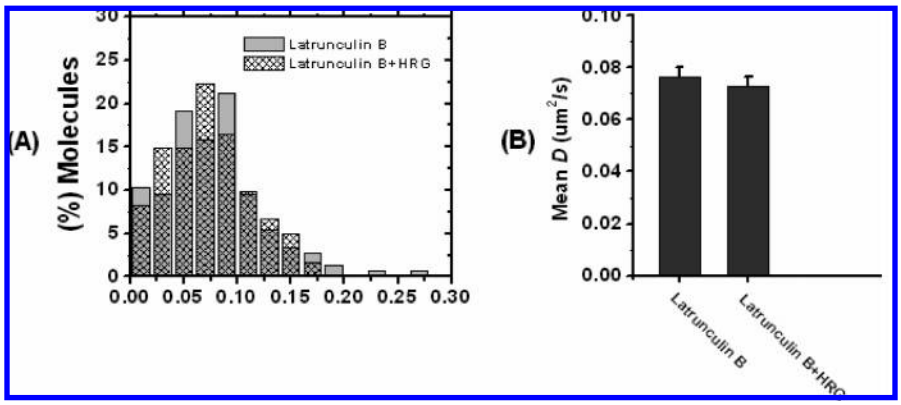

Figure 4. (A) Histograms of diffusion coefficients of individual HER2 molecules before (light gray) and after (dash) HRG stimulation in the cells treated with Latrunculin B. The mean diffusion coefficients were 0.077 ± 0.0038 and 0.073 ± 0.0036 $\mu m^2/s$ respectively. No significant difference was found between the two distributions ($p > 0.05$) as shown in part B.

Correlation between the Increased Mobilty of HER2 and Receptor Phosphorylation. The following question is why HER2 was more mobile after stimulation. We further examined whether the inhibition of tyrosine phosphorylation of the receptor would affect HER2 mobility in the presence of HRG. Figure 3E showed that, although HER2 phosphorylation was blocked by adding its specific tyrosine kinase inhibitor, the HER2 molecules still displayed the similar diffusion behavior after HRG stimulation as that before (mean value from 0.085 ± 0.0032 to 0.077 ± 0.0047 $\mu m^2/s$, $p > 0.05$). However, if both tyrosine kinase inhibitors of HER2 and EGFR were added, the diffusion of HER2 substantially slowed down (mean from 0.085 ± 0.0032 to 0.037 ± 0.0038 $\mu m^2/s$, $p < 0.001$, Figure 3F). Moreover, the tyrosine kinase inhibitor of EGFR alone had no effect on the diffusion of the activated HER2 (mean from 0.085 ± 0.0032 to 0.082 ± 0.0051 $\mu m^2/s$, $p > 0.05$, Figure 3D). Our results indicated that either the phosphorylation of HER2 or EGFR would cause the faster diffusion of HER2 after HRG stimulation.

The analysis of the size change in HER2 diffusion confinement domain showed the consistent results with that of the *D* change. For example, if the tyrosine phosphorylation of either EGFR or HER2 took place by HRG stimulation, HER2 diffused within a microdomain of 0.97 ± 0.029 or 0.91 ± 0.019 μm, which was larger than that in the resting state (0.64 ± 0.018 μm). Only under the condition that the tyrosine phosphorylations of both EGFR and HER2 were prevented, the diffusion diameter decreased significantly (0.36 ± 0.0020 μm). As both HER2 and EGFR are the heteromerization partners of HER3, treating the cells with HRG might induce an increase in the tyrosine phosphorylation of not only transfected HER2 and but also endogenous EGFR.[9,32] Therefore, the inhibition of tyrosine phosphorylation of one receptor is not enough to inhibit HRG signaling and HER2 diffusion change. Thus, the increased mobility of HER2 upon HRG stimulation is correlated with the tyrosine phosphorylation of HER2 or EGFR.

The change in receptor mobility is often caused by the change in the local membrane environment, where many factors such as cytoskeleton, lipid rafts, or adaptor molecules are involved. Therefore, it is expected that the HRG signaling by either tyrosine phosphorylation of HER2 or EGFR would alter the local environment of HER2, which facilitates its diffusion. Adam et al. reported that HRG stimulation resulted in an enhancement of F-actin expression, membrane ruffling, and cell migration.[5] Thus cytoskeletal reorganization upon HRG activation is a possible reason for the HER2 mobility change. We have tested the cells treated with LatrunculinB, a toxin that distrupts the actin cytoskeleton.[30] As shown in Figure 4, no obvious change was found in the *D* distribution before and after activation ($p > 0.05$), indicating that HRG stimulation did not lead to HER2 mobility change in those cells. We also observed that F-actin disrupting by Latrunculin B treatment resulted in the increase of HER2 mobility in rest cells (mean value is from 0.055 ± 0.0035 to 0.077 ± 0.0038 $\mu m^2/s$), which was different from the previous report.[25] It is possibly due to different F-actin disrupting reagent and different cell line used in our experiment. In this study, we only concerned HER2 diffusion change before and after HER2 simulation in the cells after F-actin disrupting. On the basis of these observations in Figure 4, we expected that, upon HRG stimulation, the cytoskeletal reorganization was initiated by either HER2 or EGFR phosphorylation, which speeded the diffusion of HER2. However, the detailed mechanism of how the receptor phosphorylation and cytoskeletal reorganization resulted in the increase of HER2 mobility needs further investigation.

Conclusion

We have imaged single molecules of GFP-tagged HER2 in living cells and characterized their diffusion mobility under different conditions. Our results showed the heterogeneity in the diffusion behavior of individual HER2 molecules, and, more importantly, the faster diffusion upon HRG stimulation and the tyrosine phosphorylation of HER2 or EGFR. It is proposed that the increase in HER2 mobility correlates with the reorganization of cytoskeleton.

Acknowledgment. The authors thank Dr. Qiang Wang and Prof. Ye-Guang Chen (Department of Biological Sciences and Biotechnology, Tsinghua University, People's Republic of China) for technical assistance in the DNA plasmid construction and Dr. Jun Wang (Institute of Chemistry, Chinese Academy of Sciences, Beijing, People's Republic of China) for the computer program in statistical analysis. This work was supported by National Natural Science Foundation of China (Nos. 30490174, 90713024, and 10334100), the National Basic Research Program of China (2007CB935601) and Chinese Academy of Sciences.

Supporting Information Available: Supporting information is available free of charge via the Internet at http://pubs.acs.org.

References and Notes

(1) Yarden, Y.; Sliwkowski, M. X. *Nat. Rev. Mol. Cell Biol.* **2001**, *2*, 127−137.
(2) Reese, D. M.; Slamon, D. J. *Stem Cells* **1997**, *15*, 1−8.

(3) Slamon, D. J.; Godolphin, W.; Jones, L. A.; Holt, J. A.; Wong, S. G.; Keith, D. E.; Levin, W. J.; Stuart, S. G.; Udove, J.; Ullrich, A. *Science* **1989**, *244*, 707−712.
(4) Way, T.-D.; Kao, M.-C.; Lin, J.-K. *J. Biol. Chem.* **2004**, *279*, 4479−4489.
(5) Adam, L.; Vadlamudi, R.; Kondapaka, S. B.; Chernoff, J.; Mendelsohn, J.; Kumar, R. *J. Biol. Chem.* **1998**, *273*, 28238−28246.
(6) Hellyer, N. J.; Kim, M. S.; Koland, J. G. *J. Biol. Chem.* **2001**, *276*, 42153−42161.
(7) Fedi, P.; Pierce, J. H.; Di Fiore, P. P.; Kraus, M. H. *Mol. Cell. Biol.* **1994**, *14*, 492−500.
(8) Chan, S. D.; Antoniucci, D. M.; Fok, K. S.; Alajoki, M. L.; Harkins, R. N.; Thompson, S. A.; Wada, H. G. *J. Biol. Chem.* **1995**, *270*, 22608−22613.
(9) Casalini, P.; Iorio, M. V.; Galmozzi, E.; Menard, S. *J. Cell. Physiol.* **2004**, *200*, 343−350.
(10) Xie, X. S.; Trautman, J. K. *Annu. Rev. Phys. Chem.* **1998**, *49*, 441−480.
(11) Byassee, T. A.; Chan, W. C. W.; Nie, S. M. *Anal. Chem.* **2000**, *72*, 5606−5611.
(12) Ueda, M.; Sako, Y.; Tanaka, T.; Devreotes, P.; Yanagida, T. *Science* **2001**, *294*, 864−867.
(13) Yao, G.; Fang, X.; Yokota, H.; Yanagida, T.; Tan, W. *Chem.−Eur. J.* **2003**, *9*, 5686−5692.
(14) Seebacher, C.; Hellriegel, C.; Bräuchle, C.; Ganschow, M.; Wöhrle, D. *J. Phys. Chem. B* **2003**, *107*, 5445−5452.
(15) Hellriegel, C.; Kirstein, J.; Bräuchle, C.; Latour, V.; Pigot, T.; Olivier, R.; Lacombe, S.; Brown, R.; Guieu, V.; Payrastre, C.; Izquierdo, A.; Mocho, P. *J. Phys. Chem. B* **2004**, *108*, 14699−14709.
(16) Slaughter, B. D; Bieber-Urbauer, R. J.; Johnson, C. K. *J. Phys. Chem. B* **2005**, *109*, 12658−12662.
(17) Schob, A.; Cichos, F. *J. Phys. Chem. B* **2006**, *110*, 4354−4358.
(18) Murakoshi, H.; Iino, R.; Kobayashi, T.; Fujiwara, T.; Ohshima, C.; Yoshimura, A.; Kusumi, A. *Proc. Natl. Acad. Sci. U.S.A.* **2004**, *101*, 7317−7322.
(19) Douglass, A. D.; Vale, R. D. *Cell* **2005**, *121*, 937−950.
(20) Iino, R.; Koyama, I.; Kusumi, A. *Biophys. J.* **2001**, *80*, 2667−2677.
(21) Vrljic, M.; Nishimura, S. Y.; Brasselet, S.; Moerner, W. E.; McConnell, H. M. *Biophys. J.* **2002**, *83*, 2681−2692.
(22) Harms, G. S.; Cognet, L.; Lommerse, P. H. M.; Blab, G. A.; Kahr, H.; Gamsjäger, R.; Spaink, H. P.; Soldatov, N. M.; Romanin, C.; Schmidt, Th. *Biophys. J.* **2001**, *81*, 2639−2646.
(23) Vrljic, M.; Nishimura, S. Y.; Moerner, W. E.; McConnell, H. M. *Biophys. J.* **2005**, *88*, 334−347.
(24) Deich, J.; Judd, E. M.; McAdams, H. H.; Moerner, W. E. *Proc. Natl. Acad. Sci. U.S.A.* **2004**, *101*, 15921−15926.
(25) Orr, G.; Hu, D.; Ozcelik, S.; Opresko, L. K.; Wiley, H. S.; Colson, S. D. *Biophys. J.* **2005**, *89*, 1362−1373.
(26) Ma, X. Y.; Wang, Q.; Jiang, Y. X.; Xiao, Z. Y.; Fang, X. H.; Chen, Y. G.; *Biochem. Biophys. Res. Commun.* **2007**, *356*, 67−71.
(27) Mukhin, Y. V.; Garnovsky, E. A.; Ullian, M. E.; Garnovskaya, M. N. *J. Pharmacol. Exp. Ther.* **2003**, *304*, 968−977.
(28) Murillo, H.; Schmidt, L. J.; Tindall, D. J. *Cancer Res.* **2001**, *61*, 7408−7412.
(29) Chen, X.; Levkowitz, G.; Tzahar, E.; Karunagaran, D.; Lavi, S.; Ben-Baruch, N.; Leitner, O.; Ratzkin, B. J.; Bacus, S. S.; Yarden, Y. *J. Biol. Chem.* **1996**, *271*, 7620−7629.
(30) Chowdhury, I.; Chaqour, B. *Eur. J. Biochem.* **2004**, *271*, 4436−4450.
(31) Kusumi, A.; Sako, Y.; Yamamoto, M. *Biophys. J.* **1993**, *65*, 2021−2040.
(32) Hutcheson, I. R.; Knowlden, J. M.; Madden, T.-A.; Barrow, D.; Gee, J. M. W.; Wakeling, A. E.; Nicholson, R. I. *Breast Cancer Res. Treat.* **2003**, *81*, 81−93.
(33) Fujiwara, T.; Ritchie, K.; Murakoshi, H.; Jacobson, K.; Kusumi, A. *J. Cell Biol.* **2002**, *157*, 1071−1081.
(34) Lommerse, P. H. M.; Blab, G. A.; Cognet, L.; Harms, G. S.; Snaar-Jagalska, B. E.; Spaink, H. P.; Schmidt, T. *Biophys. J.* **2004**, *86*, 609−616.